Passive Attitude Damping of Alternative Assembly Configurations of Space Station Freedom

James W. Wade*
University of Colorado, Boulder, Colorado 80309

Because of the large size of the proposed U.S. Space Station Freedom, a difficulty exists pertaining to the manifest of initial assembly flights. A fully functioning vehicle with communication, control, and reboost capability would be ideal. As a result of the size and weight of Freedom's components, the Space Shuttle is unable to deliver a fully functioning vehicle without the use of heavy, expensive, temporary components such as avionics, propulsion, and control. An alternative lies in the use of passive magnetic dampers.

I. Introduction

THE proposed U.S. Space Station Freedom (Fig. 1) will require several Space Shuttle flights to complete. The assembly sequence and the content of each flight are very critical to ensure efficient delivery and construction of Freedom. The present first flight manifest would leave in orbit a less than desirable configuration from a stability and control point of view. This prospect has prompted a study of gravity gradient stable, passively damped, alternate configurations.

The November 1988 baseline flight 1 configuration (Fig. 2) consists of four bays of truss, the assembly work platform (AWP), a starboard photovoltaic module, a reaction control system (RCS), and a temporary avionics pallet.[1] The first flight attempts to provide active attitude control and orbit reboost using the RCS jets. This flight has several undesirable qualities, including short orbit lifetime in a passive flight mode, limited fuel supply, gravity gradient instability, no backup control system, and the need for a costly, throwaway avionics package.

A study was conducted that introduced alternate flight 1 configurations that have attitude oscillations passively damped by a spherical magnetic damper. Three alternative flight 1 configurations are proposed, henceforth referred to as case 1, case 2, and case 3. Case 1 consists of the same components as the baseline configuration; however, the solar arrays and radiator are not extended (Fig. 3). Case 2 consists of the same components as the baseline configuration, but only the solar arrays are stowed (Fig. 4). Case 3 consists primarily of two resource nodes (Fig. 5). All three alternate flights proposed are gravity gradient stable, are passively damped by a magnetic damper, have high ballistic coefficients for longer orbit lifetimes, and permit the baseline assembly sequence to continue after flight 4. A spherical magnetic damper, when used with gravity gradient stable spacecraft, is an effective, inexpensive, and lightweight method of reducing attitude oscillations.

This report investigates the operation, effectiveness, and size of a spherical magnetic damper when used on the alternative configurations. Characteristics of a good vehicle for passive damping are mentioned, and afterwards the operation and design of magnetic dampers is presented. The damper coefficient and its effect on spacecraft performance are then mentioned. The advantages and limitations of multiple dampers are discussed, followed by the derivation of the torque provided by a magnetic damper. A model of the geomagnetic field and the simulation used to verify the effectiveness of a magnetic damper is explained, as are the performance analysis methods and results.

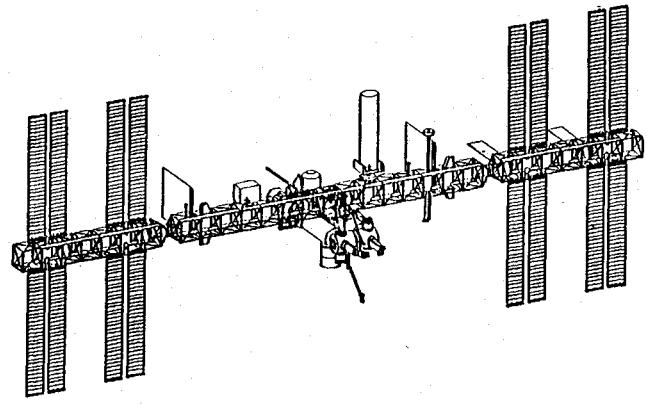

Fig. 1 U.S. Space Station Freedom.

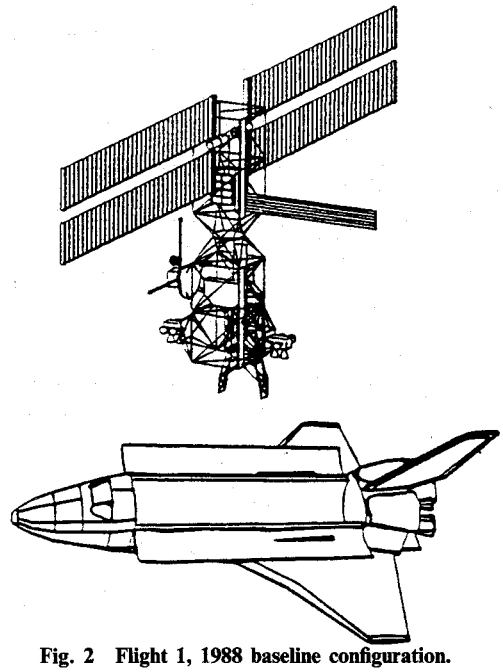

Fig. 2 Flight 1, 1988 baseline configuration.

Received July 20, 1989; presented as Paper 89-3435 at the AIAA Guidance, Navigation, and Control Conference, Boston, MA, Aug. 14–16, 1989; revision received Nov. 17, 1989.

*Research Assistant, Aerospace Engineering Department. Member AIAA.

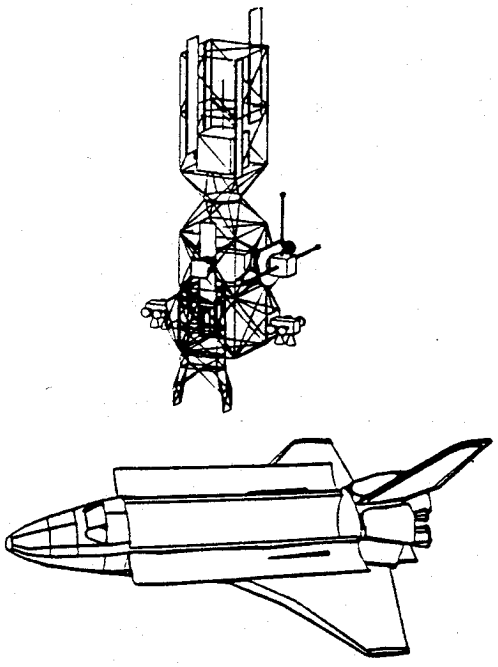

Fig. 3 Flight 1, case 1.

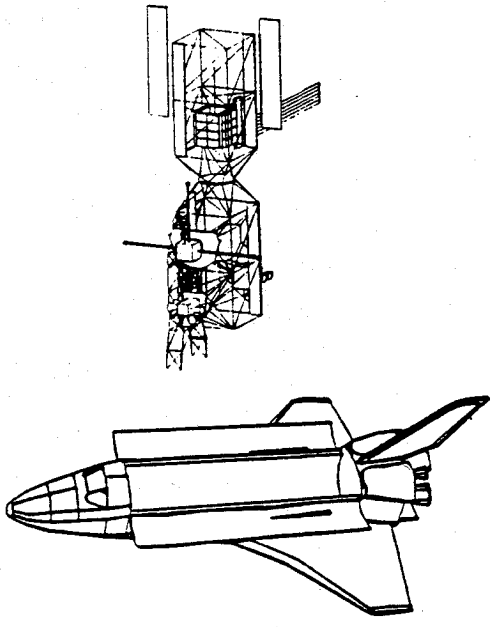

Fig. 4 Flight 1, case 2.

II. Vehicle Configuration

The vehicle configuration is a primary consideration when using a magnetic damper. A good configuration would be a gravity gradient stable, compact vehicle with low fluctuation in aerodynamic torque.

A gravity gradient stable configuration is one in which the moment of inertia about pitch is the largest and the moment of inertia about yaw is the smallest ($I_{\text{pitch}} > I_{\text{roll}} > I_{\text{yaw}}$). A typical, although not optimal, ratio would be approximately 7 : 6 : 2.

The magnitude of the moments of inertia has a direct impact on the size of the magnetic damper, since a given damping torque will have a greater effect on a small moment of inertia. A compact vehicle will require a smaller damper than a configuration of the same mass that is spread out (i.e., one resource node vs about 10 bays of constructed truss).

Another driver of vehicle configuration is the impact of aerodynamic torques. A passive vehicle will oscillate about the trim attitude or torque equilibrium attitude (TEA) of the vehicle. The TEA is the attitude at which the environmental, gravity gradient, and gyroscopic torques are equal. As a result of changing atmospheric density, this attitude will change throughout the orbit as the vehicle passes from night to day. The damper must be able to reduce the oscillations caused by these aerodynamic disturbance torque fluctuations in order to provide attitude damping to the vehicle. The magnitude of the aerodynamic torque fluctuations, and thus the size of the damper, rapidly increases in the presence of asymmetric aerodynamic torques due to solar arrays, radiators, and so forth.

III. Magnetic Damper Operation

Magnetic dampers, developed by General Electric ASTRO Space Division, have been used for passive attitude damping in several satellites, including the Geodetic Earth Orbiting Satellite, the Geodynamics Experimental Ocean Satellite, the Gravity-Gradient Test Satellite, the Timeation Satellite, and the Long Duration Exposure Facility. Several Naval Research Laboratory satellites also use magnetic dampers for passive attitude damping.[2]

A magnetic damper consists of two concentric spheres. The inner sphere contains a permanent magnet that aligns itself with the Earth's magnetic field lines, and the outer sphere is attached to the spacecraft body (Fig. 6). Between the spheres is a viscous fluid for the viscous damper, or a diamagnetic material for the eddy current damper. In either case the resulting damping torque is the product of the relative angular velocity between the two spheres and the damping coefficient of the damper. The damping coefficients for both types of magnetic dampers are expressed as follows.[3]

Eddy current damper:

$$K_d = (u_o M)^2 \sigma r^5 S \tag{1}$$

where

u_o = permeability of free space
M = magnet strength

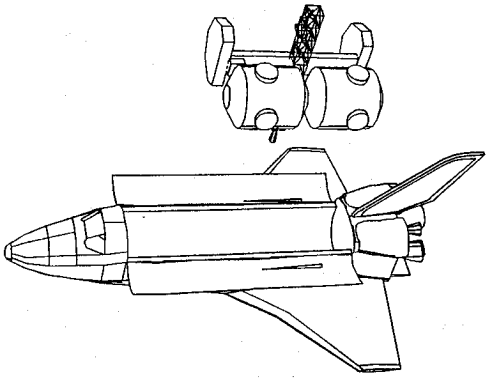

Fig. 5 Flight 1, case 3.

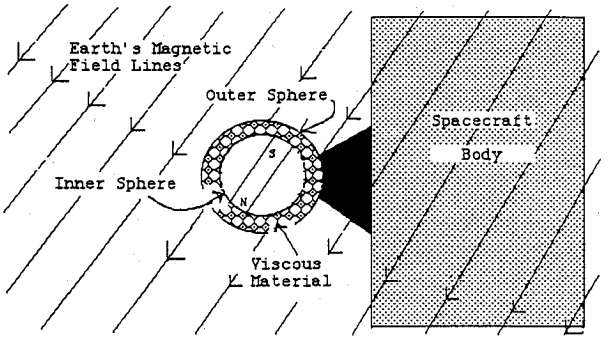

Fig. 6 Magnetic damper.

σ = conductivity of diamagnetic material
r = radius of sphere
S = shape factor

Viscous damper:

$$K_d = \frac{8\pi u_o r^4}{3\epsilon_o} \tag{2}$$

where
u_o = viscosity of fluid
r = radius of sphere
ϵ_o = spacing between spheres

Dampers that require a damping coefficient between 1 and 5 N-m-s generally are of the viscous type, whereas those with coefficients less than 1 N-m-s are of the eddy current type.

The attitude response of the spacecraft due to the damper is determined by the damper coefficient, whereas the effectiveness of the damper is dependent on the aligning capability, or strength of the inner magnet.

A standard magnetic damper with a damper coefficient greater than 5 N-m-s provides a damping torque large enough that the inner magnet deviates significantly from the Earth's magnetic field orientation. This results in the inner sphere and magnet being dragged along by the spacecraft oscillations instead of the inner sphere applying a damping torque to the spacecraft. Thus, a damper coefficient limit of 5 N-m-s per standard-sized dampers is established unless very strong inner magnets are available.

Figure 7 clarifies the effect of the inner magnet size on the damping time by plotting the damping time vs the damping parameter of a magnetic damper. The damping parameter is the dimensionless ratio of the damping coefficient to the product of the pitch moment of inertia and the orbital frequency. The magnet parameter is the ratio of the magnet strength to the spacecraft pitch moment of inertia and adjusts the damping time depending on the inner magnet strength. The diagonal represents a magnet parameter of infinity, which implies that an infinitely strong inner magnet is being used.

For example, if a spacecraft has a damping parameter of 0.04 and desires a damping time of 8 orbits, a magnet parameter of 10 is required. This has about the same effect as if an infinite magnet were used. However, if a magnet parameter of 5 were used, the damping time would increase to about 12 orbits.

The physical dimensions of a standard magnetic damper are approximately the same for dampers with coefficients less than 5 N-m-s. All standard-sized dampers have a weight of approximately 22 lb and a diameter under 1 ft. In addition, an optional 3-ft-diam sphere surrounding the damper provides protection against magnetic contamination. Small ferric particles may be attracted to the magnetic field of the damper and attach to the outer space, thereby disturbing the inner magnet and degrading damper performance. The foam sphere could help prevent this magnetic contamination and also prevent devices such as the extravehicular maneuvering unit (EMU) from coming too close to the damper and thus being exposed to magnetic fields that are larger than allowable.

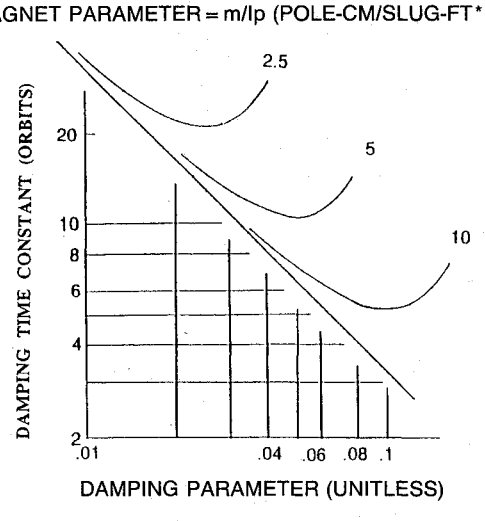

Fig. 7 Effect of damping parameter and damping time constant on magnet parameter.

IV. Damper Coefficient Size

The material between the spheres of the magnetic damper, either viscous or eddy current, is determined by the damping coefficient and the environment in which the damper will be operating. For standard-sized viscous dampers, all parameters in Eq. (2) are constant with the exception of the viscosity u_o. Damper coefficients ranging from 1 to 5 N-m-s may be obtained from a standard damper by varying the fluid viscosity. A variety of viscous, silicon-type materials exist that provide a given viscosity throughout a specified thermal operating range for viscous dampers.

An optimally sized damper coefficient for a particular spacecraft configuration is one that reduces the steady-state oscillations yet provides fast damping times. Steady-state oscillations, as used here, are the damper-induced oscillations resulting from the particular solution of the differential equations of motion. Damping time is the time for the attitude oscillations to decay to $1/e$ of their original oscillations after a disturbance is imposed on the configuration.

Large damping coefficients will decrease damping times at the expense of larger steady-state errors brought about by disturbance torques from the inner magnet tracking the relative position of the Earth's magnetic field. Disturbance torques from the inner magnet of the damper are not as pronounced when less than optimal damper coefficients are utilized; therefore, steady-state oscillations decrease at the expense of increased damping times. Thus, the optimal coefficient is the coefficient that provides an overall optimal response, yet neither damping time nor steady-state oscillations may be optimized.

The optimal damper coefficient may be calculated mathematically or experimentally with the use of computer simulation. Mathematical solutions are straightforward for polar circular orbits with a simple magnetic field model.[4] However, the solution becomes increasingly difficult as more general orbits and an accurate model of the Earth's magnetic field are considered. Iteration with a computer simulation was used to solve the problem with the 28.5-deg inclination orbit of Freedom by assigning a damping time of approximately 24–36 h.

A damping time of 24–36 h was chosen so that if upon an attempted berthing with the passive vehicle on a later flight a disturbance was imposed on the vehicle, the Orbiter may be able to wait for any oscillations to dampen before another berthing attempt. A time of 24–36 h was chosen as the maximum amount of time the crew would be able to wait and still perform the assembly objectives of that assembly flight.

V. Multiple Dampers

Combining several standard dampers with small damping coefficients on a spacecraft will result in a total effective damping coefficient equal to the sum of the individual damping coefficients. This presents an effective method for achieving a system redundancy along with an effective damping coefficient larger than the 5 N-m-s limit for a single damper.

The economical break-even point for using several standard-sized dampers as opposed to designing and manufacturing one large, special damper is about 10 standard-sized dampers. It is better to use five standard dampers instead of one damper that is five times as large as a standard damper. However, it is better to build one damper 15 times larger than

a standard damper instead of using 15 standard-sized dampers. The break-even point is established by the availability of the standard dampers and the projected costs associated with the special manufacture and design of a large damper.

Multiple dampers may be placed either on truss pieces or on the AWP. A distance of approximately 12 ft should be maintained between standard dampers, with no less than a 2-ft separation from magnetic materials or current loops.

VI. Magnetic Damper Torque

The torque T^d produced by a spherical magnetic damper may be represented as the product of the damper coefficient K_d and the relative angular velocity between the inner and outer spheres ω^r:

$$T^d = -K_d \omega^r \tag{3}$$

The relative angular velocity is the difference between the outer sphere (satellite) angular velocity ω^o and the inner sphere (magnet) angular velocity ω^i:

$$\omega^r = \omega^o - \omega^i \tag{4}$$

The angular velocity of the inner sphere, assuming perfect tracking of the geomagnetic field lines by the magnet, is the angular velocity of the Earth's magnetic field unit vector. Restoring torques exist that align the inner magnet axis with the Earth's magnetic field. However, no torque exists to restrict the inner magnet from rotating about the Earth's magnetic field lines. Therefore, no torque is applied about the geomagnetic field lines, since the inner magnet will simply rotate about these lines. The inner sphere angular velocity may be written as

$$\omega^i = b \times \frac{db}{dt} + (\omega^o \cdot b)b$$

$$= b \times Q + (\omega^o \cdot b)b \tag{5}$$

where

b = unit vector of the magnetic field, B
Q = components of the derivative of b with respect to time
$(\omega^o \cdot b)b$ = spacecraft (and consequently the inner magnet) angular velocity about the Earth's magnetic field

Because of the rotating frame of the spacecraft, Q may be written as

$$Q = q + \omega^o \times b \tag{6}$$

where q is introduced to represent the derivative of the components of b, and ω^o is the angular velocity of the spacecraft.

The angular velocity of the inner sphere may now be rewritten by substituting Eq. (6) into Eq. (5):

$$\omega^i = b \times (q + \omega^o \times b) + (\omega^o \cdot b)b$$

$$= b \times q + \omega^o - (\omega^o \cdot b)b + (\omega^o \cdot b)b \tag{7}$$

The torque exerted on the satellite by the damper may be represented in spacecraft coordinates by substitution of Eq. (4) into Eq. (3):

$$T^d = K_d(\omega^i - \omega^o) \tag{8}$$

The total damping torque exerted on the spacecraft in spacecraft coordinates may now be found from Eqs. (7) and (8):

$$T^d = K_d b \times q \tag{9}$$

The assumption that the inner sphere is anchored to the geomagnetic field lines is valid if the damping constant is sized so that the damping torque is smaller than the torque required to cause large displacements of the inner sphere from its magnetic field orientation. This also implies that the inner magnet is large enough to maintain its magnetic field orientation in order to attain reasonable damping times.

Magnetic dampers provide only two-axis damping at any instant in time, with no torque in the direction of the Earth's magnetic field. For orbit inclinations of 28.5 deg as with Freedom, this results in poor pitch damping, since the magnetic field lines are generally perpendicular to the orbit plane.

VII. Inner Sphere Dynamics

The inner sphere angular velocity ω^i may also be determined by modeling the inner sphere dynamics. The dynamics of the inner sphere of the magnetic damper may be written as

$$[J]\dot{\omega}^i + [\omega^i][J]\omega^i = T^B + T^d \tag{10}$$

where

$[J]$ = inertia matrix of the inner sphere
ω^i = angular velocity of the inner sphere
$[\omega^i]$ = skew symmetric matrix representing $w^i x$
T^B = torque of the inner magnetic dipole in the Earth's magnetic field
T^d = damping torque on vehicle

Since $[J]$ of the 7-lb inner magnet and ω^i are small, Eq. (10) may be approximated by

$$T^B = -T^d \tag{11}$$

The inner magnetic attempts to remain aligned with the Earth's magnetic field, but as a damping torque is applied to the spacecraft, an equal torque is applied to the inner magnet-Earth field system. The steady-state response of the magnet to a constant torque is governed by

$$T^d = -mB \sin\theta \tag{12}$$

where

T^d = damping torque magnitude
m = magnetic dipole moment magnitude
B = Earth magnetic field vector
θ = deflection angle between the magnetic dipole moment vector and the geomagnetic field vector

Computer simulation results have shown that modeling the inner sphere dynamics by Eq. (11) produces comparable results to the modeling of the entire inner sphere dynamics of Eq. (10). Computer simulations also showed that similar results were obtained for a perfectly tracking inner sphere [Eq. (9)], when the inner magnet strength was calculated after the computer simulation.

The inner magnet strength, or dipole moment, may be found from Eq. (11) by assuming a maximum deflection of 20 deg of the inner magnet:

$$m = \frac{T^d}{B \sin 20} \tag{13}$$

The magnitude of the damping torque and the Earth's magnetic field may be calculated numerically throughout a computer simulation. The numerical results may be used to calculate the size of the inner magnet dipole moment after a simulation. The number of standard magnetic dampers required for a particular configuration may be approximated by dividing the result of Eq. (13) by the dipole moment of a standard magnetic damper, 225 A-m^2.

Table 1 Transient variations of the Earth's magnetic field

Disturbance	Variation	Angular change, rad	Duration, min	Angular rate, rad/s
Diurnal effect	100γ	4×10^{-3}	180	4×10^{-7}
Magnetic storm				
Sudden commencement	50γ	2×10^{-3}	2	2×10^{-5}
Initial phase	600γ	2×10^{-2}	180	2×10^{-6}
Hydrodynamic wave	100γ	4×10^{-3}	1	7×10^{-5}
Other disturbances	5γ	1×10^{-4}	0.167	1×10^{-5}
Maximum perturbation of field	855γ	3×10^{-2}		1×10^{-4}

VIII. Earth's Magnetic Field Model

At distances below 10 Earth radii, the geomagnetic field is similar to a magnetic dipole, which is slightly offset from the Earth's rotation axis. The field may be accurately modeled, so that it may support a magnetic damper model in a 6-DOF simulation, by using a spherical harmonic representation of the field.[5]

The geomagnetic field, or the Earth's $\boldsymbol{B}$ field, may be written as the negative gradient of the scalar potential V:

$$\boldsymbol{B} = -\text{grad}\, V \tag{14}$$

in which

$$V(r,\theta,\Phi) = a \sum_{n=1}^{k} \left(\frac{a}{r}\right)^{n+1} \left\{ \sum_{m=0}^{n} [g_n^m \cos(m\Phi) + h_n^m \sin(m\Phi)] P_n^m(\theta) \right\} \tag{15}$$

where

a = Earth's radius
g_n^m, h_n^m = Gaussian coefficients
k = order of field model
$P_n^m(\theta)$ = associated Legendre functions
r = distance from the Earth's center
θ = coelevation (measured southward from true north)
Φ = longitude from Greenwich

Therefore,

$$B_r = \sum_{n=1}^{k} (n+1) \left(\frac{a}{r}\right)^{n+2} \left\{ \sum_{m=0}^{n} [g_n^m \cos(m\Phi) + h_n^m \sin(m\Phi)] P_n^m(\theta) \right\} \tag{16}$$

$$B_\theta = -\sum_{n=1}^{k} \left(\frac{a}{r}\right)^{n+2} \left\{ \sum_{m=0}^{n} [g_n^m \cos(m\Phi) + h_n^m \sin(m\Phi)] \frac{\delta P_n^m}{\delta t}(\theta) \right\} \tag{17}$$

$$B_\Phi = \frac{1}{\sin\theta} \sum_{n=1}^{k} \left(\frac{a}{r}\right)^{n+2} \left\{ \sum_{m=0}^{n} [m g_n^m \sin(m\Phi) - h_n^m \cos(m\Phi)] P_n^m(\theta) \right\} \tag{18}$$

where

B_r = component of the field in the direction of increasing radius (up)
B_θ = component in the direction of increasing colatitude (south)
B_Φ = component in the direction of increasing longitude from Greenwich (east)

The accuracy of the magnetic field model is affected by the number of terms, k, in the summation. The $k = 1$ term characterizes the dipole strength and orientation, the $k = 2$ term varies the quadrapole value, and so on, with each n defining more individual segments of the field.

IX. Earth's Magnetic Field Changes

The Earth's magnetic field may change slightly as a result of secular and transient variations.[6] The secular changes represent very slow variations, less than 0.1% per year in most locations and up to 0.3% per year in some areas. The source of the secular drift may be attributed to the internal drift of the geomagnetic dipole moment. These changes may be accounted for in the spherical harmonic representation [Eq. (16–18)] by adjusting the Gaussian coefficients by measurable drift rates.

Transient variations result from external sources and are much more variable than secular variations. These variations are caused primarily by solar electromagnetic radiation and charge particles from the sun. The main variations occur in the form of diurnal variations and magnetic storms.

Diurnal variations are caused by tidal motions induced in the ionosphere by solar heating. This variation is most noticeable near the equator, where, over several hours, the Earth's field may increase by as much as 100γ.

The Earth's magnetic field magnitude is about $25{,}000\gamma$ at low Earth orbit. Higher latitudes experience a decrease of about 50γ.

Variation due to magnetic storms are most noticeable during the sudden storm commencement (ssc) and the initial phase. During the ssc a rapid increase in the horizontal component of the Earth's field occurs ($\Delta B \sim 50\gamma$). The initial phase is marked by a decrease of several hundred gamma or more with a duration from a few minutes to several hours.

Other transient variations result from hydrodynamic waves, auroral-type fluctuations, micropulsations, and extra-low-frequency phenomena such as seasonal variations. In general, these effects have less of an effect on the geomagnetic field than the diurnal variations and magnetic storms.

Table 1 summarizes the predominant magnetic disturbances encountered in a low Earth orbit with an inclination of 28.5 deg. The worst-case values of variation, response time, angular change, and angular rate for each disturbance are listed. The angular change is calculated by applying the disturbance perpendicular to the lowest expected value of the Earth's field. The angular velocity is determined by dividing the angular change by the response time of the disturbance. The maximum perturbation to the Earth's magnetic field is calculated by summing the individual, worst-case disturbances.

The maximum perturbation to the Earth's field is approximately 855γ, resulting in a maximum angular change of about 3×10^{-2} rad (1.7 deg) and an angular velocity of 1×10^{-4} rad/s. If the maximum disturbance of 855γ were to be applied parallel to the Earth's field, its magnitude would change by about 3%.

Gravity gradient stable spacecraft generally oscillate with a frequency on the order of orbital frequency (1×10^{-3} for low Earth orbit). Also, the decrease in the damping torque that can be applied to the spacecraft is directly proportional to the magnitude of the Earth's magnetic field. Effects due to the transient variations in the Earth's magnetic field were neglected, since the worst-case angular rate of the magnetic field variation is an order of magnitude smaller than the attitude oscillation rate, and the worst-case decrease in damping torque is only 3%.

The worst-case values would only occur, at most, once a year during solar maximum. Nominal fluctuations are at least an order of magnitude smaller than the worst case values. The true driver of damper disturbance torques does not come from geomagnetic variations, but from the much more predominant aerodynamic torque in low Earth orbit.

X. Space Systems Integrated Simulation

The attitude response of the baseline and alternate configurations was determined with the use of the Space Systems Integrated Simulation (SPASIS). SPASIS is a generic 6-DOF, on-orbit simulation for investigating the behavior and interaction of the variety of subsystems that can make up a spacecraft.

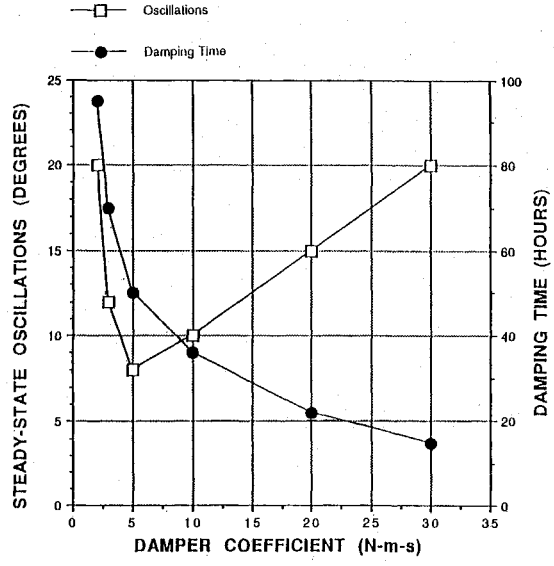

Fig. 8 Case 1, initialized 20-deg yaw, pitch, roll offset, steady-state oscillations, and damping time vs damper coefficient.

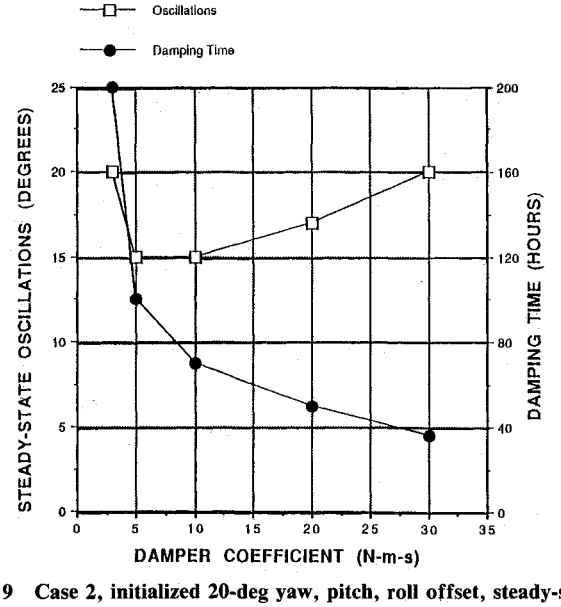

Fig. 9 Case 2, initialized 20-deg yaw, pitch, roll offset, steady-state oscillations, and damping time vs damper coefficient.

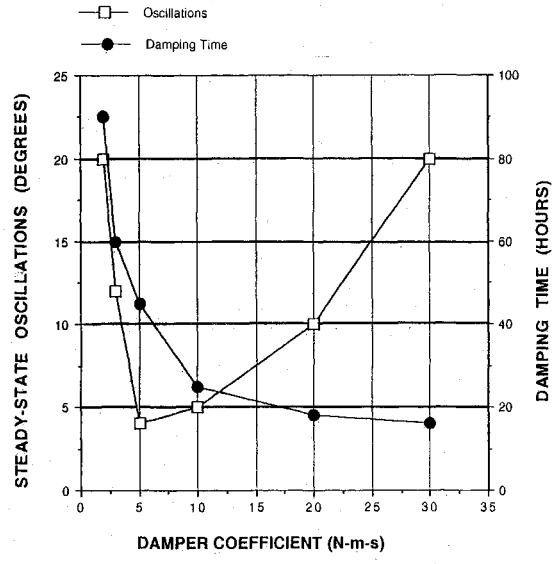

Fig. 10 Case 3, initialized 20-deg yaw, pitch, roll offset, steady-state oscillations, and damping time vs damper coefficient.

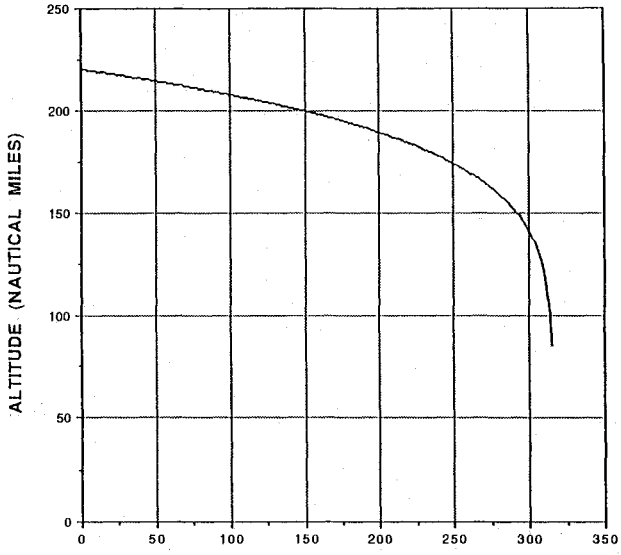

Fig. 11 Case 1 orbital lifetime.

The Earth's magnetic field is modeled in the environment using Eqs. (16–18), and the magnetic damper is modeled in the control system using Eq. (9). Both models were verified in a previous study.[7]

XI. Performance Analysis

The analysis, which was conducted on the flight 1 configurations, included an initial deflection analysis and an orbit lifetime comparison. Each configuration was initialized with an equal angular deflection about yaw, pitch, and roll axes, respectively. The attitude response was observed to identify the decrease in oscillations over 30 orbits. The initial deflections were imposed after the configuration was placed in the TEA. Using SPASIS, the dynamic analyses were performed on each configuration with several damper coefficients and without a magnetic damper. The orbital lifetimes of the alternate configurations were calculated by the simulation DAYPLOT.

The calculation of orbit altitude by DAYPLOT requires user input of orbital and environment parameters as well as the spacecraft projected areas. Because of the relatively stable attitudes of the alternate configurations, the projected area calculation presented no difficulty. However, the large oscillations of the baseline flight exposed different areas of the configuration to aerodynamic influences. One of these areas consists primarily of the solar arrays and truss; the second consists primarily of the radiator and truss. The orbit lifetime with each projected area was calculated, and the two lifetimes were averaged to obtain the baseline flight orbit lifetime.

All analyses were conducted assuming an early 1994 launch date, 220-n. mi. altitude, an upper 2σ atmosphere, and the Earth's magnetic field expanded to the octupole term [$k = 3$ in Eqs. (16–18)].

XII. Results

To establish data for different damping coefficients, the simulations were limited to a time of about 45 h. Cases 1 and 3 showed favorable responses with a reasonably sized, 10 N-m-s damper. Case 2 had adequate damping with a large 30 N-m-s damper. The passively damped baseline flight had an unfavorable response when equipped with a very large 300.0 N-m-s damper.

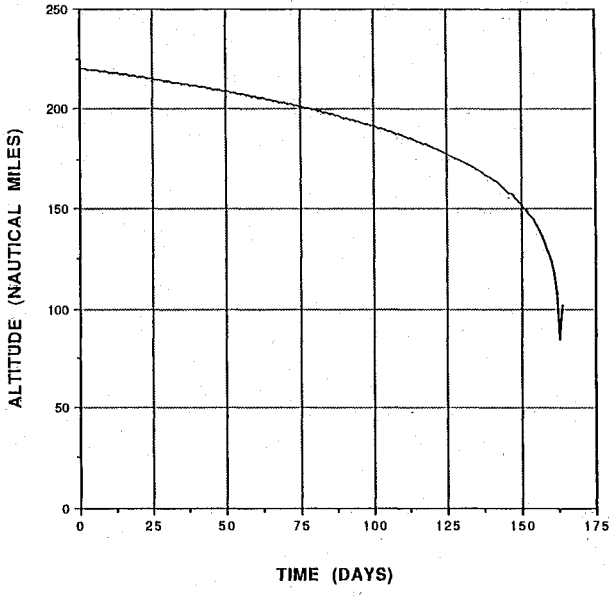

Fig. 12 Case 2 orbital lifetime.

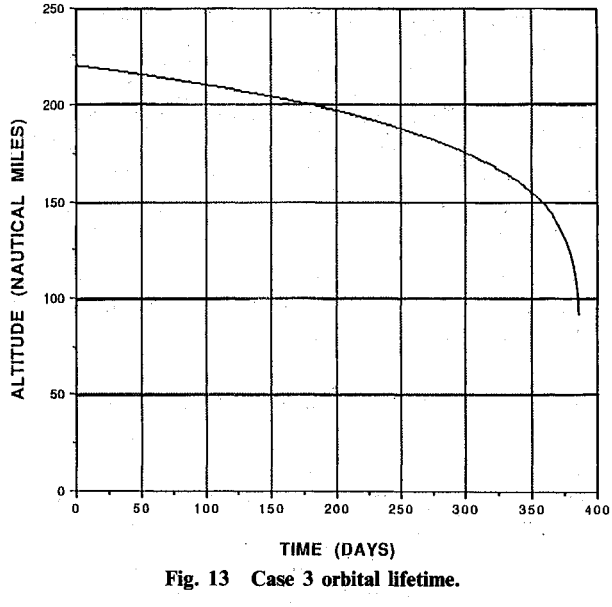

Fig. 13 Case 3 orbital lifetime.

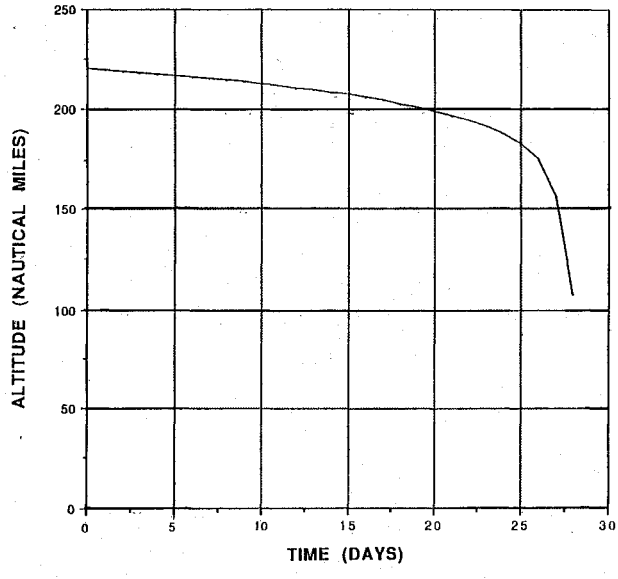

Fig. 14 Baseline configuration orbital lifetime.

Steady-state oscillations and damping times for various damper coefficients are displayed in Figs. 8–10 when the alternate configurations are initialized with offsets from TEA of 20 deg in yaw, pitch, and roll. As a result of double scaling of the plots, the optimal damper coefficient does occur at crossing of the lines. Rather, the plots were used to compare damping times with various damper coefficients. The steady-state oscillations, which may be expected, were then read from the same graph.

Case 1 was able to recover from an initial deflection of 20 deg in yaw, pitch, and roll and regain a stable attitude in under 36 h. Computer simulation results showed that approximately seven standard-sized dampers, each with a damper coefficient of 1.4 N-m-s, could supply the required damping. The orbit lifetime of case 1 was calculated by DAYPLOT to be approximately 300 days (Fig. 11).

Case 2 was able to recover from an initial deflection of 20 deg in yaw, pitch, and roll and regain a stable attitude in under 36 h. One special damper, 13 times stronger than a standard damper and weighing several hundred pounds, could provide the required damping with a damper coefficient of 30 N-m-s. Case 2 has an orbital lifetime of approximately 150 days (Fig. 12).

Case 3 was able to recover from an initial deflection of 20 deg in yaw, pitch, and roll and regain a stable attitude in under 30 h. Six standard-sized dampers, each with a damper coefficient of 1.67 N-m-s, could provide the damping. The orbit lifetime of case 3 was calculated by DAYPLOT to be approximately 375 days (Fig. 13).

A very massive damper with a coefficient of 300.0 N-m-s was determined to be the smallest coefficient that would reduce oscillations for the baseline flight 1 configuration. This large damper coefficient requirement results from the fact that the damping torque must be able to reduce the oscillations caused by the aerodynamic disturbance torque. This only occurs if the damper coefficient for the baseline configuration is greater than 300 N-m-s. Large steady-state oscillations that exist for the baseline configuration are the result of the large damper coefficient and the influence of large fluctuation in aerodynamic torque. For the passive baseline configuration the orbit lifetime, as calculated by DAYPLOT, is approximately 25 days (Fig. 14). This short lifetime is due to a large area-to-weight ratio of the passive baseline flight configuration.

The increase in required damping coefficient from case 1 to case 2 is caused, to a small extent, by the slight increase in the moments of inertia. The primary reason for the increase is the influence of aerodynamic torques due to the thermal radiator. The thermal radiator produces small aerodynamic torques when the flight is initialized in the TEA. However, once a slight yaw offset is given to the configuration, the oscillations begin to grow and then shrink as the attitude oscillations of the vehicle move in and out of phase with the aerodynamic density variations as the vehicle orbits the Earth.

XIII. Conclusion

Spherical magnetic dampers are a proven, reliable, and lightweight method for achieving passive attitude damping on highly gravity gradient stable, low aerodynamic profile spacecraft. The alternate flight 1 configurations meet these criteria of gravity gradient stability and low aerodynamic profile. Magnetic dampers, when used on the alternate configurations, present effective and efficient options for the initial assembly flights of the U.S. Space Station.

Acknowledgment

This work was performed for the Program Engineering Office of the NASA Johnson Space Center under Contract NAS-9-17900 while the author was a Senior Associate Engineer in the Advanced Programs Department of Lockheed Engineering & Sciences Company, Houston, Texas.

References

[1]"Space Station Freedom Program Level II, System Engineering and Integration (SE&I) Assembly Sequence CR BB 000468 Supporting Data," NASA, Rept. SSE-E-88-R20, Washington, DC, Sept. 1988.

[2]Repass, G. D., Lerner, G. D., Coriell, K. P., and Legg, J. S., Jr., "Geodynamics Experimental Ocean Satellites (GEOS-C) Prelaunch Report," NASA Rept. X-580-75-23, Feb. 1975.

[3]Breedlove, W., and Heinbockel, J., "A Formulation of the Equations of Motion for the Long Duration Exposure Facility (LDEF)," Old Dominion Univ., Norfolk, VA, TR-74-M3, Sept. 1974.

[4]Lerner, G. M., "Autonomous Attitude Stabilization Systems," *Spacecraft Attitude Determination and Control*, edited by J. Wertz, Reidel, Boston, MA, 1986, Sec. 18.3.

[5]Plett, M., "Magnetic Field Models," *Spacecraft Attitude Determination and Control*, edited by J. Wertz, Reidel, Boston, MA, 1986, Appendix H.

[6]Chernosky, E. J., Fougere, P. F., and Hutchinson, R. O., "The Geomagnetic Field," *Handbook of Geophysics and the Space Environment*, edited by A. S. Jursa, Air Force Space Command, USAF, 1985, Chap. 11.

[7]Wade, J. W., "Spherical Magnetic Dampers," Lockheed, Houston, TX, TR-LEMSCO-24352, June 1988.